Enhancement of Single-Molecule Fluorescence Using a Gold Nanoparticle as an Optical Nanoantenna

Sergei Kühn, Ulf Håkanson, Lavinia Rogobete, and Vahid Sandoghdar*
Laboratory of Physical Chemistry, ETH Zurich, CH-8093 Zurich, Switzerland
(Received 1 December 2005; published 7 July 2006)

We investigate the coupling of a single molecule to a single spherical gold nanoparticle acting as a nanoantenna. Using scanning probe technology, we position the particle in front of the molecule with nanometer accuracy and measure a strong enhancement of more than 20 times in the fluorescence intensity simultaneous to a 20-fold shortening of the excited state lifetime. Comparisons with three-dimensional calculations guide us to decipher the contributions of the excitation enhancement, spontaneous emission modification, and quenching. Furthermore, we provide direct evidence for the role of the particle plasmon resonance in the molecular excitation and emission processes.

DOI: 10.1103/PhysRevLett.97.017402 PACS numbers: 78.67.Bf, 07.79.Fc, 33.80.−b, 42.50.−p

Metals are notorious for quenching the radiation of emitters placed in their near field [1–3]. On the other hand, it is known that the luminescence [4,5] and Raman signals can be enhanced on metallic nanostructures [6–9]. The desire to understand and exploit these phenomena has triggered a large number of investigations over more than three decades [10–12]. However, quantitative measurements and comparisons with theoretical predictions have been plagued by the lack of control over the large number of parameters that determine the radiation properties of an emitter close to a nanostructure. To address this challenging issue, we have studied the interaction of a single oriented molecule with a single spherical gold nanoparticle under *in situ* position control [see Fig. 1(a)].

A gold nanoparticle (GNP) supports plasmon resonances associated with the excitation of a collective oscillation of electrons. The scattering properties and the plasmon spectra of small GNPs are well described in the quasistatic dipole approximation limit of Mie theory if one takes into account radiation damping [13,14]. Thus, given a dipolar radiation pattern and a well-defined resonance spectrum, a GNP behaves as an elementary resonant dipole antenna. In what follow, we investigate the strong influence of such a nanoantenna on the excitation and emission of a single molecule (SM).

Let us consider an emitter with ground and excited states $|g\rangle$ and $|e\rangle$ placed at the origin. The fluorescence signal detected from the emitter is given by $S_f = \xi\sigma_{ee}\gamma_r$, where ξ is the overall detection efficiency of the setup, σ_{ee} is the population of the excited state, and γ_r is its radiative decay rate. To obtain σ_{ee}, one should consider the effects of saturation and triplet bottle neck but in the regime well below saturation, where all measurement in this work were performed, $S_f \propto \xi|\langle e|\mathbf{E}.\mathbf{D}|g\rangle|^2\eta$. Here $\eta = \gamma_r/(\gamma_r + \gamma_{\mathrm{nr}})$ denotes the fluorescence quantum efficiency whereby γ_{nr} is the nonradiative decay rate of $|e\rangle$. The excitation electric field at the location of the molecule is represented by $\mathbf{E}$, and $\mathbf{D}$ stands for molecular dipole moment operator. Now if we introduce a nanostructure at $\mathbf{r} = (x, y, z)$ with r being much smaller than the transition wavelength, the molecule experiences an inhomogeneous $\mathbf{E}$ field so that the excitation rate becomes a very sensitive function of $\mathbf{r}$ and the molecular orientation. Moreover, the vicinity of the nanostructure alters both γ_r and γ_{nr} in a strongly distance and orientation dependent manner [15–17]. To make the matter more complicated, all these processes depend on the correspondence between the possible plasmon resonances of the nanostructure and the molecular excitation and emission wavelengths λ_{exc} and λ_f, respectively. For a given

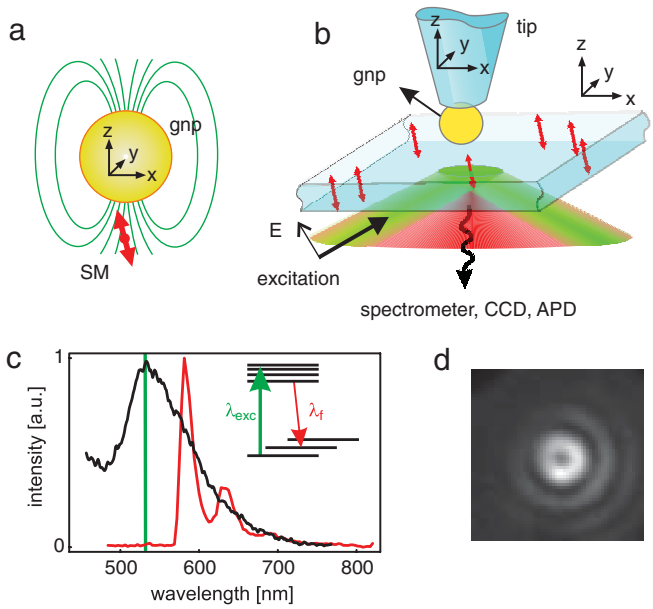

FIG. 1 (color). (a) The main idea of our work: a single gold nanoparticle (GNP) is scanned across a single molecule. The green lines sketch the inhomogeneous excitation field. (b) The schematics of the experimental arrangement. (c) The black curve shows the measured plasmon spectrum of a GNP attached to the glass fiber tip. The red curve displays the emission spectrum of terrylene. The sharp short wavelength edge is due to the cutoff filter. The green line marks the excitation wavelength at 532 nm. (d) A CCD camera image of an SM in the absence of a GNP.

nanostructure and a molecular dipole moment of certain orientation we rewrite S_f as

$$S_f \propto \xi I_0 d_{eg}^2 K(\mathbf{r}, \lambda_{\mathrm{exc}}) \eta(\mathbf{r}, \lambda_f), \quad (1)$$

where K represents the excitation process and accounts for the enhancement of the electric field intensity near the nanostructure as well as its projection onto the direction of $\mathbf{D}$. The quantities I_0 and d_{eg} stand for the incident excitation intensity in the absence of the nanostructure, and for the matrix element associated with the g-e transition.

The experimental setup consists of a scanning shear-force stage [14,18,19] mounted on an inverted optical microscope [see Fig. 1(b)]. Uncoated heat-pulled fiber tips carrying single GNPs (diameter 100 nm) at their extremities were prepared according to the recipe reported in Ref. [18]. The plasmon spectrum of the GNP attached to the tip was monitored by dark-field illumination with white light from a xenon lamp through the microscope objective [14]. The black curve in Fig. 1(c) displays the plasmon resonance of a typical GNP. The sample was a 20–30 nm thin para-terphenyl (pT) crystalline film doped with a very low concentration (10^{-9} molar) of terrylene molecules, obtained from spin coating [20]. An important advantage of this system is that the pT matrix is thin enough to allow near-field studies. Furthermore, terrylene molecules are oriented almost parallel to the z axis, possess near unity quantum efficiency and are remarkably photostable [19,20]. In addition, as indicated in Fig. 1(c), the excitation wavelength and fluorescence spectra of terrylene nicely overlap with the GNP plasmon resonance, allowing us to investigate the role of the latter in the modification of both excitation and emission enhancement processes.

Terrylene molecules were excited by a pulsed laser at a wavelength of $\lambda_{\mathrm{exc}} = 532$ nm with a pulse width of less than 30 ps. A p-polarized laser beam was offset from the center of the microscope objective (numerical aperture of 1.4) so as to achieve total internal reflection at the pT-air interface and to adapt the polarization of the excitation light to the molecular dipole orientation in the film. A sensitive CCD camera was used to identify individual fluorescent molecules in a wide-field image of the sample [20]. Figure 1(d) shows an example of an SM image. The slight asymmetry in the doughnut-shaped pattern allows us to determine the orientation of terrylene molecules in pT films to be about $15 \pm 5°$ with respect to the substrate normal [19]. In what follows we take the position of a given molecule to be at $x = y = 0$ and $z = z_0$ whereby the sample-air interface is set at $z = 0$. To couple the GNP to single terrylene molecules, the tip was approached to the pT sample and distance stabilized at a separation of the order of 1 nm using shear-force control. The GNP was next scanned laterally across various molecules, allowing us to visualize directly a strong increase of the molecular fluorescence on the camera. An example movie can be found at the online supplementary materials [21]. Then an SM was selected and positioned at the center of the field of view, and its fluorescence light was directed through a pinhole onto an avalanche photodiode (APD) in a confocal detection arrangement. The output of the APD was fed to a time card which was synchronized with the arrival time of the laser pulses. By recording the arrival time of each photon with respect to the laser pulse, we determined the excited state decay time (τ) of the molecule. For terrylene τ is about 4 ns in bulk pT, but it increases for molecules with perpendicular orientation close to the pT-air interface [19]. In our samples we measured $\tau_0 \simeq 20$ ns in the absence of the GNP.

Figure 2(a) shows S_f from an SM under constant illumination, as the GNP was scanned laterally nearly in contact with the sample surface. Here the blue background represents the fluorescence signal S_f^0 of the molecule in the absence of the GNP. In this measurement, the molecule was photobleached shortly after the GNP passage, providing us with a direct measure of the small residual fluorescence of the system. Figure 2(b) displays S_f/S_f^0 for a cross section of Fig. 2(a) after subtracting this residual fluorescence [22]. We find that in this run S_f is enhanced by up to

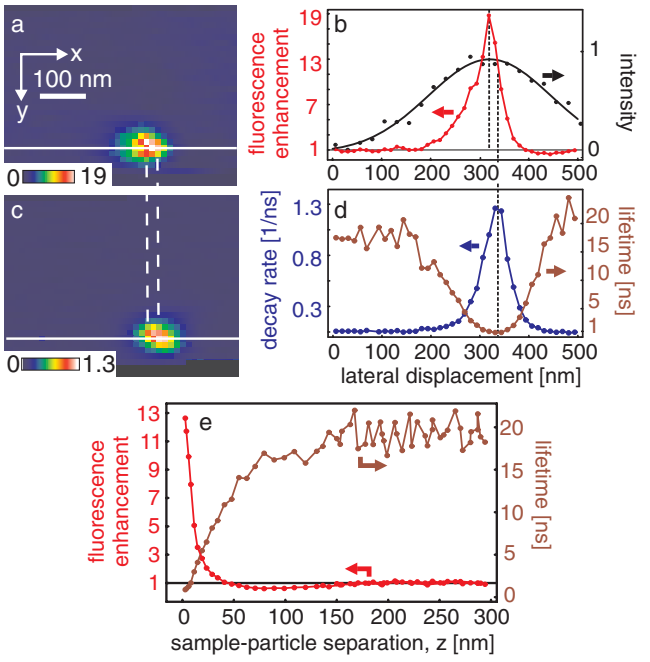

FIG. 2 (color). (a) Normalized fluorescence signal of an SM as a function of the lateral position of the GNP placed nearly in contact with the sample. (b) The red curve shows a cross section from (a) after subtraction of a small background fluorescence. The black curve displays, for comparison, a confocal fluorescence signal as the molecule was scanned through a focused laser beam (without the tip). (c) Lateral position dependence of the fluorescence decay rate recorded simultaneously as in image (a). (d) The brown and blue curves show the fluorescence lifetime and the corresponding decay rate for the same cross section shown in (b). (e) The red curve represents S_f/S_f^0 as a function of z. The brown curve shows τ measured simultaneously as S_f.

19 times when the GNP is placed in the near field of the molecule.

Figure 2(c) displays the map of the excited state decay rate $\gamma = 1/\tau$ obtained simultaneously as S_f presented in Fig. 2(a). The blue (brown) curve in Fig. 2(d) shows γ (τ) from the same cut as in Fig. 2(a). Here we find that γ increases by up to 22 times when the GNP was scanned over the molecule. However, note that as marked by the vertical dashed lines in Figs. 2(a)–2(d), the excellent signal-to-noise ratio of the data reveals a small lateral shift of about 20 nm between the maxima of S_f and γ. Furthermore, there is a slight asymmetry in the curves of Figs. 2(b) and 2(d). These features are due to the sensitive dependence of S_f and γ on the relative orientation and position of the molecular dipole with respect to the GNP [21].

In addition to scanning the particle in the xy plane at $z \simeq 0$, we have also performed xyz scans. This is particularly useful for a quantitative analysis (discussed below) because as opposed to scans along x or y [21], the relative orientation of the molecular dipole with respect to the GNP remains constant during a z scan. The red and brown curves in Fig. 2(e) display S_f/S_f^0 and τ, respectively, as a function of z for a molecule different from the one in Figs. 2(a)–2(d). In this run a 13-fold enhancement of S_f is accompanied by a 22 times decrease (increase) of τ (γ) at the shortest molecule-GNP separation. We point out, in passing, the slight dip of the normalized fluorescence signal below one, which also occurs in Fig. 2(b). This is due to the interference between the incident laser beam and its scattering from the GNP [21,23].

The full width at half-maximum of the "image" of the molecule in Fig. 2(b) is about 65 nm, which compared to a typical confocal fluorescence scan of a molecule without the GNP (black curve) reveals the near-field improvement of the resolution. Furthermore, the data in Fig. 2(e) illustrate that the enhancement effects in the z direction are confined only to about 10 nm. In the context of optical microscopy, these demonstrate the realization of the most elementary "apertureless" near-field optical microscope [24] with a well-defined nanoscopic probe and a single-molecule sample. Note that reducing the size of the GNP would improve the resolution further.

A quantitative comparison of our experimental data with the theory requires three-dimensional calculations that take into account the effect of the pT-air interface both for the excitation and fluorescence processes. Such calculations go beyond the scope of this Letter and remain a subject of future investigations. Nevertheless, it is instructive to compare our results with the predictions of 3D calculations for γ_r and γ_{nr}, neglecting the substrate. Here we have followed the formalism presented in Ref. [16] and have considered a molecule tilted by 15° with respect to the radial axis of a GNP placed in air. We used the values of the dielectric functions of gold at $\lambda_f = 580$ nm provided by Ref. [25]. Figure 3 shows the change of γ_r (green), γ_{nr} (pink) and the total decay rate $\gamma = \gamma_r + \gamma_{nr}$ (blue), all normalized to the unperturbed decay rate γ^0 and plotted as a function of the molecule-GNP separation along the z axis. The inset shows a zoom of the short distance region and also η (black curve). To accommodate a direct comparison with the experimental data, we have also included γ from Fig. 2(e) (blue symbols). If one were to fit the blue curve to the symbols, leaving only the depth z_0 of the molecule as a free parameter, one would obtain $z_0 = -12.5 \pm 0.5$ nm. This would lead us to deduce $\eta \simeq 0.5$, $\gamma_r \simeq 11\gamma^0$, and $\gamma_{nr} \simeq 11\gamma^0$ for the closest molecule-GNP separation achieved experimentally. Furthermore, remembering that S_f has risen by about 13 times for the same measurement [Fig. 2(e)], Eq. (1) would imply that $K \approx 25$ at this separation.

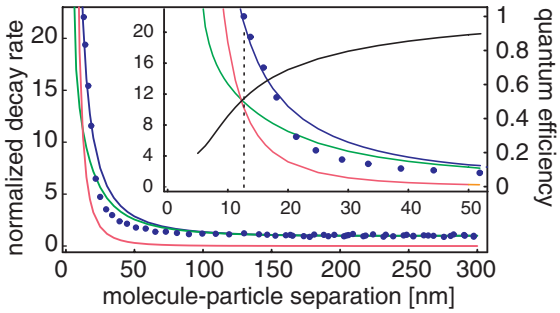

FIG. 3 (color). The green, pink, and blue curves represent the theoretical values of radiative, nonradiative and total decay rates, respectively, as normalized to the unperturbed decay rate γ^0. The symbols plot $1/\tau$ from the data in Fig. 2(e) for direct comparison. The inset shows a zoom of the closer region. The black curve displays the resulting quantum efficiency, the dashed line marks the closest molecule-GNP separation.

Within the model used here, we can also evaluate the theoretically expected intensity enhancement K, by using exact Mie theory to compute the near field of a GNP illuminated by a plane wave [13]. The inset in Fig. 4 shows examples of the near-field enhancement for two GNP-molecule separations of 2 and 12 nm. The predicted enhancement of about 5–20 is somewhat lower than the value

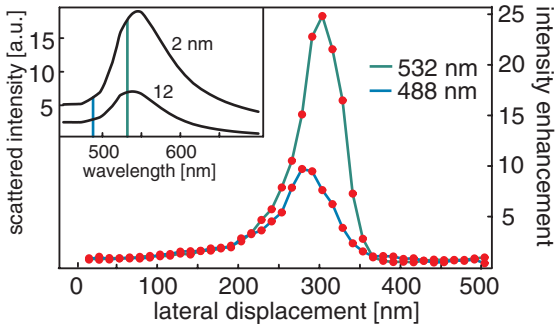

FIG. 4 (color). Green and blue curves connecting red symbols show the dependence of the fluorescence enhancement S_f/S_f^0 on the lateral molecule-GNP displacement for the same single molecule excited at $\lambda = 532$ and 488 nm, respectively. The inset shows the theoretical near-field intensity enhancement as a function of wavelength for molecule-GNP separations of 2 and 12 nm.

of $K \approx 25$ deduced above. One explanation that might come to mind is the possible change of ξ in Eq. (1) as the GNP is approached to the molecule. The movie in the online supplementary materials [21] shows that while the emission pattern of a molecule can be somewhat modified when the GNP is scanned laterally over the molecule, it is not affected in a notable manner when the GNP is above the molecule. Our calculations verify that indeed, a small round nanoparticle does not change the emission pattern of a radially oriented dipole in its near field. Furthermore, our microscope objective collects more than 75% of the fluorescence from a single molecule in a pT film supported by glass. Therefore, any redirection of fluorescence by the GNP would not result in a considerable increase of the detected signal. Thus, changes in ξ do not affect the estimation of K from the data in Figs. 2(e) and 3. We believe that the stronger excitation enhancement deduced from our data is due to the presence of the substrate. Indeed, the scattering cross section of a gold nanoparticle is increased in the vicinity of a substrate [19] and for near-field excitation [26].

We have verified that replacing the GNP with an extended metallic tip without a resonant character results in complete fluorescence quenching instead of enhancement [23]. In order to provide a direct proof of the central role of the GNP plasmon resonance in the enhancement process, we have examined the fluorescence of the same molecule (a different molecule than those studied in Fig. 2) under excitation at $\lambda = 532$ nm and 488 nm. As displayed in the inset of Fig. 4, the near-field intensities at these two wavelengths differ by a factor of about 2.5. In Fig. 4, the symbols connected by the green and blue lines show the normalized intensity S_f/S_f^0 as a function of the GNP position in the x direction for the excitation wavelengths 532 and 488 nm, respectively. We find that S_f is indeed enhanced by about 2.5 times more under green excitation, illustrating the importance of the antenna resonance in the excitation enhancement. Furthermore, comparison of the emission spectrum of a single molecule with and without the presence of a GNP also clearly reveals the influence of the plasmon spectrum on γ_r. A more detailed account of this measurement and analysis is given in the online supplementary material [21].

In conclusion, we have demonstrated a controlled enhancement of single-molecule fluorescence due to its near-field coupling with a gold nanoparticle. Moreover, we have presented a clear evidence for the role of local plasmon resonances in the excitation and emission processes. The choice of a well-characterized system and the quality of our experimental data made it possible to compare them directly with three-dimensional calculations for individual molecules, without the need for statistical averaging. We emphasize that the experimental procedure and observations presented here were repeated for many molecules and could be reproduced routinely. Our approach based on the use of a nanoantenna is also promising for various applications such as detection of weakly fluorescing systems [27].

We thank R. Carminati, I. Gerhardt, and A. Imamoglu for fruitful discussions. This work was supported by the Swiss National Foundation and the Swiss Ministry of Education and Science (EU IP-Molecular Imaging).

*Electronic address: vahid.sandoghdar@ethz.ch

[1] R. R. Chance, A. Prock, and R. Silbey, Adv. Chem. Phys. **37**, 1 (1978).
[2] X. S. Xie and R. C. Dunn, Science **265**, 361 (1994).
[3] E. Dulkeith *et al.*, Phys. Rev. Lett. **89**, 203002 (2002).
[4] K. T. Shimizu, W. K. Woo, B. R. Fisher, H. J. Eisler, and M. G. Bawendi, Phys. Rev. Lett. **89**, 117401 (2002).
[5] J. Farahani, D. W. Pohl, H.-J. Eisler, and B. Hecht, Phys. Rev. Lett. **95**, 017402 (2005).
[6] S. Nie and S. R. Emory, Science **275**, 1102 (1997).
[7] K. Kneipp *et al.*, Phys. Rev. Lett. **78**, 1667 (1997).
[8] R. M. Stöckle, Y. D. Suh, V. Deckert, and R. Zenobi, Chem. Phys. Lett. **318**, 131 (2000).
[9] N. Hayazawa, Y. Inouye, Z. Sekkat, and S. Kawata, Chem. Phys. Lett. **335**, 369 (2001).
[10] M. Moskovits, Rev. Mod. Phys. **57**, 783 (1985).
[11] A. Hartschuh, A. B. M. Beversluis, and L. Novotny, Phil. Trans. R. Soc. A **362**, 807 (2004).
[12] J. A. Dieringer *et al.*, Faraday Discuss. **132**, 9 (2006).
[13] U. Kreibig and M. Vollmer, *Optical Properties of Metal Clusters* (Springer, Berlin, 1995).
[14] T. Kalkbrenner, U. Håkanson, and V. Sandoghdar, Nano Lett. **4**, 2309 (2004).
[15] R. Ruppin, J. Chem. Phys. **76**, 1681 (1982).
[16] P. C. Das and A. Puri, Phys. Rev. B **65**, 155416 (2002).
[17] M. Thomas, J.-J. Greffet, R. Carminati, and J. R. Arias-Gonzalez, Appl. Phys. Lett. **85**, 3863 (2004).
[18] T. Kalkbrenner, M. Ramstein, J. Mlynek, and V. Sandoghdar, J. Microsc. **202**, 72 (2001).
[19] B. C. Buchler, T. Kalkbrenner, C. Hettich, and V. Sandoghdar, Phys. Rev. Lett. **95**, 063003 (2005).
[20] R. J. Pfab *et al.*, Chem. Phys. Lett. **387**, 490 (2004).
[21] See EPAPS Document No. E-PRLTAO-97-002627 for a discussion of (1) Modification of the single-molecule emission spectrum, (2) asymmetry of the simultaneously recoded lateral images of γ and S_f, and (3) modification of the single-molecule emission pattern, including an online movie. For more information on EPAPS, see http://www.aip.org/pubservs/epaps.html.
[22] When the GNP enters the evanescent field of the excitation light at the air-pT interface, it fluoresces by a very small amount. However, since this signal is weak and constant, we can account for it without any complications.
[23] S. Kühn and V. Sandoghdar, Appl. Phys. B (to be published).
[24] F. Zenhausern, M. P. O'Boyle, and H. K. Wickramasinghe, Appl. Phys. Lett. **65**, 1623 (1994).
[25] P. B. Johnson and R. W. Christy, Phys. Rev. B **6**, 4370 (1972).
[26] M. Quinten, A. Pack, and R. Wannemacher, Appl. Phys. B **68**, 87 (1999).
[27] M. D. Barnes *et al.*, J. Phys. Chem. B **104**, 6099 (2000).